JOURNAL OF Materials CHEMISTRY

Electrodeposited lithium phthalocyanine thin films. Part II:† magnetic properties and mesoscopic effects

M. Brinkmann* and J.-J. André

Institut Charles Sadron, 6, rue Boussingault, 67083 Strasbourg cédex, France. E-mail: martin@ism1.ism.bo.cnr.it

Received 16th December 1998, Accepted 16th April 1999

The magnetic properties of lithium phthalocyanine thin films obtained by electrodeposition onto ITO glass substrates are investigated *via* electron paramagnetic resonance (EPR). These properties are shown to depend on several parameters such as (i) the electrolysis time (t_e), which controls the size of the crystallites as well as their unidirectional ordering in the thin films and (ii) the nature of the solvent used during electrodeposition. Highly oriented x-form thin films of thickness *ca.* 2 μm ($t_e \approx 30$ min) exhibit similar properties as observed for single crystals: (i) a narrow EPR signal with a linewidth in the range 20–30 mG which broadens linearly with the oxygen pressure and (ii) a low dimensional behaviour of the linewidth anisotropy. A correlation is found between the mean size of the microcrystallites in the thin films and the EPR signal linewidth according to the equation $\Delta H_{pp} = K\langle l \rangle^{\alpha}$, where K is a constant and $\alpha \approx 0.38 \pm 0.04$. The temperature dependence of the EPR signal linewidth and the magnetic susceptibility are analyzed in terms of spin $S = 1/2$ solitons which are thermally generated with a typical activation energy $E_a(\chi)$ of *ca.* 0.04–0.06 eV.

1 Introduction

Among all the metallophthalocyanines, the lithium phthalocyanine radical (PcLi) exhibits an intrinsic semiconducting behaviour and some peculiar magnetic properties.[1] This monomolecular organic semiconductor can crystallize in three different structures, namely the x, α and β structures, depending on the synthesis route.[2,3] A detailed electron paramagnetic resonance (EPR) study of these three polymorphs has evidenced very different magnetic properties strongly correlated to the molecular packing.[4] It has been shown that only the x-form powders and single crystals exhibit a very narrow EPR signal under vacuum ($\Delta H_{pp} \approx 20$–70 mG) which broadens proportionally to the partial pressure of oxygen.[5] The angular dependence of the EPR signal linewidth (single crystal) is characteristic of a one dimensional system, with a maximum linewidth observed when the stacking axis (long axis of the crystallite) is oriented parallel to the Zeeman field and two minima located close to the magic angles (*ca.* $\pm 55^{\circ}$ on each side of the maximum). These magnetic properties are closely related to the tetragonal crystal structure of PcLi (x-PcLi). The PcLi molecules are stacked into well separated columns (interstack distance *ca.* 1.40 nm) in a face-to-face configuration with an intermolecular distance in the stacks of *ca.* 0.321 nm which leads to strong intra-stack π-orbital overlaps. Diffusion channels located along the stacking axis (*c* axis) of the x structure allow oxygen molecules to diffuse in the bulk and then to act as traps for the diffusing/delocalised spins of PcLi. The magnetic exchange interactions between the $S = 1$ spins of O_2 and the $S = 1/2$ spins of PcLi lead to a linear dependence between the EPR signal linewidth and the oxygen pressure (the sensitivity factor $d(\Delta H_{pp})/dP(O_2)$ is *ca.* 5 G bar^{-1}).[5] The x structure of PcLi is therefore believed to be a good candidate for use in devices suitable for both oximetry and magnetometry.[6] However, a synthetic route to unidirectionally oriented x-PcLi thin films is required to achieve this goal.

Oriented PcLi thin films have been obtained *via* high-vacuum deposition onto various inorganic substrates such as glass, KBr or mica.[7,8] Structural studies of these thin films revealed a peculiar polymorphism which is intimately related to the deposition conditions. However, even though x-PcLi thin films have been obtained, their corresponding magnetic properties are quite different from those observed *via* EPR in powders and single crystals.[9] In particular, the EPR signals of vacuum deposited thin films are much broader ($\Delta H_{pp} \approx 0.8$–$1.0$ G) compared to those of single crystals and powders because of the localized nature of the spins.

Recently, a new synthetic route based on the electrodeposition of PcLi thin films onto ITO substrates has been proposed.[10] We demonstrated the possibility of controlling the mean microcrystallite size in a large range (0.3–500 μm) by simple tuning of the electrolysis time (from a few seconds to about 30 min). This allowed us to investigate size effects on the intrinsic magnetic properties of x-PcLi. Films obtained when $t_e < 1$ min in acetonitrile show a random distribution of needle-shaped crystallites lying with their *c* axis (stacking axis) in the plane of the substrate. For longer electrolysis times, the needle-shaped microcrystallites of up to 500 μm in length form interconnected bundles which tend to align along one preferential direction in the plane of the ITO substrate, which is denoted the *c* axis hereafter.[10] The morphology of thin films grown in acetone is quite different: the films show a smaller surface coverage (*ca.* 50 microcrystallites per 100 μm^2) and no unidirectional ordering of the crystallites because of their curved shape, clearly observed when $t_e > 5$ min.

The aim of the present study is to investigate the magnetic properties of these electrodeposited PcLi thin films by means of EPR. In particular, we focus on the relationship existing between the growth conditions, such as the electrolysis time or the solvent used during synthesis, and the corresponding magnetic properties. Accordingly, the overall magnetic properties of x-PcLi are analyzed in the framework of a soliton model.

2 Experimental

2.1 Thin film preparation

The method used for PcLi thin film growth is based on the electrochemical oxidation of $PcLi_2$ as reported for the synthesis of x-PcLi powders and single crystals.[1,10] The thin film electrosynthesis was performed in a three-electrode, two-compartment cell sectioned off by means of a fritted glass disk (porosity 4). The working electrodes (anode) consisted of indium tin

†Part I: ref. 10.

oxide (ITO) conducting glass purchased from Glastron Inc. (surface resistance of *ca.* 20 Ω □$^{-1}$). The substrates were initially sonicated in a 1 : 1 ethanol–acetone solution for several minutes and subsequently dried in a nitrogen flow. A $PcLi_2$ solution with a concentration of approximately 10^{-4} M was prepared by diluting 50 μl of a $PcLi_2$ solution ($[PcLi_2]=0.1$ M in pentanol, Europhthal) in 50 ml of acetone or acetonitrile. The conducting salt concentration was in the range $1–5\times10^{-2}$ M. Electrochemical syntheses were performed in the presence and the absence of an inert gas (nitrogen or argon). Similar magnetic and structural properties were obtained in both cases. The working potential (Bruker E130M potentiostat) of *ca.* 0.4 V *vs.* SCE was applied during a time lapse in the range 5 s–30 min and was measured *versus* a saturated calomel electrode. After reaction, the $PcLi_2$ solution was gently removed from the electrochemical cell avoiding any agitation. The films were subsequently dried in ambient atmosphere in an oven at 50 °C for several minutes in order to remove any traces of solvent.

2.2 EPR characterization

All the spectra were recorded under vacuum at low microwave power (*ca.* 2 μW) with a low modulation amplitude (*ca.* 6 mG) and a low frequency (*ca.* 12.5 kHz) in order to avoid saturation, distortion and side bands, respectively. Multiple scanning was performed using the field frequency lock to avoid any experimental broadening of the narrow EPR signals. Low temperature characterization of the samples was performed using a Bruker ER300 spectrometer equipped with a TE_{102} cavity and an Oxford ESP300 cryostat.

Samples of x-PcLi on an ITO substrate of typical size 2×2 mm were fixed onto a Teflon holder using EPR silent Apiezon grease. In order to study the intrinsic magnetic properties of the thin films (4–300 K), the samples were kept under vacuum in sealed quartz tubes ($P<10^{-3}$ Torr). The temperature of the samples was controled by means of a thermocouple (AuFe (0.3%)–Chromel) held in the vicinity of the quartz tube. The *g*-factor was obtained from direct measurements of the magnetic field at resonance with an NMR gaussmeter and the microwave frequency (X band) using an HP5053B frequency counter. The microwave field H_1 was calibrated using a tetracene solution in concentrated sulfuric acid.

For both the kinetic study of oxygen diffusion in the x-form thin films and the linewidth anisotropy at 300 K, we used a Bruker ESP300E spectrometer which allows for an automatic spectrum acquisition at a high acquisition rate of about 0.2–0.3 Hz. In order to avoid any linewidth broadening of the very narrow EPR signals, we used a field frequency lock during multiple scanning. The magnetic field homogeneity and/or stability for the ER300 spectrometer is *ca.* 30 mG whereas for the ESP300E spectrometer it is better than 4 mG ($\Delta g/g<10^{-5}$).

In order to reduce the noise to signal ratio, we calculated the linewidth anisotropy from the peak-to-peak amplitude anisotropy $A_{pp}(\theta)$, assuming a constant line shape so that $\Delta H_{pp}\propto1/\sqrt{A_{pp}}$. It must however be stressed that the EPR signal of a 1D system is a Lorentzian only at the magic angles, *i.e.* for $\theta=\pm55°$. Nevertheless, the linewidth anisotropies of the half-width at half maximum $\Delta H_{1/2}(\theta)$ and of the peak-to-peak amplitude $A_{pp}(\theta)$ are nearly identical which justifies the previous approximation.

The anisotropy of the EPR signal in the Zeeman field was checked in two different planes namely a plane containing the *c* axis and another one which is perpendicular to the *c* axis. Accordingly, the samples were rotated around two different axes: (i) an axis which is perpendicular to the *c* axis, as illustrated in Fig. 6 and (ii) around the *c* axis itself, as shown in Fig. 8.

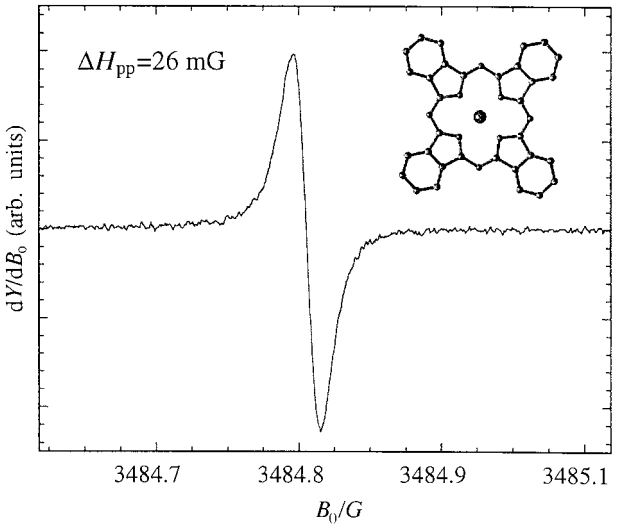

Fig. 1 EPR absorption spectrum at 300 K for an x-form PcLi thin film of thickness *ca.* 2 μm obtained *via* electrodeposition onto an ITO glass substrate in acetonitrile ($t_e=30$ min). The film was kept under primary vacuum and oriented at the magic angle to the Zeeman field (the *c* axis is at 55° relative to B_0). The inset shows a schematic view of a PcLi molecule ($C_{32}N_8H_{16}Li$).

3 Results

3.1 Magnetic properties at 300 K

3.1.1 Effect of the electrolysis time (films grown in acetonitrile). The intrinsic magnetic properties of x-form PcLi thin films obtained by electrodeposition onto ITO glass are quite different from those reported for vacuum deposited films. Indeed, as seen in Fig. 1, thin films obtained after electrolysis times of *ca.* 30 min exhibit a narrow Lorentzian-like EPR signal under vacuum at $g\approx2.00214$ with a typical peak-to-peak linewidth ΔH_{pp} in the range 17–30 mG, which is similar to that reported for x-PcLi single crystals ($\Delta H_{pp}\approx25$ mG).[5] As seen in Fig. 2, both the linewidth and the line shape of the

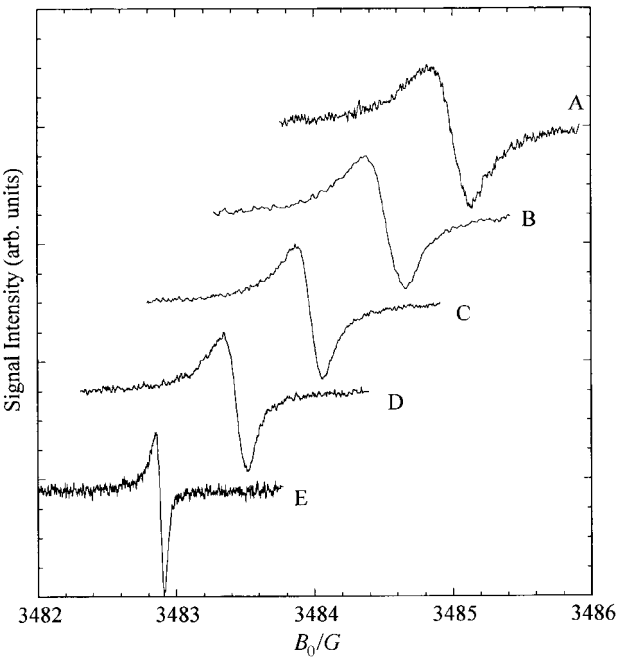

Fig. 2 EPR spectra at 300 K for x-PcLi electrodeposited films grown in acetontrile onto ITO substrates for increasing electrolysis times: (A) $t_e=5$ s, (B) $t_e=10$ s, (C) $t_e=20$ s, (D) $t_e=40$ s and (E) $t_e=2$ min. The films were all kept under primary vacuum and oriented at the magic angle to the Zeeman field. The spectra have been shifted along both the magnetic field axis and the intensity axis.

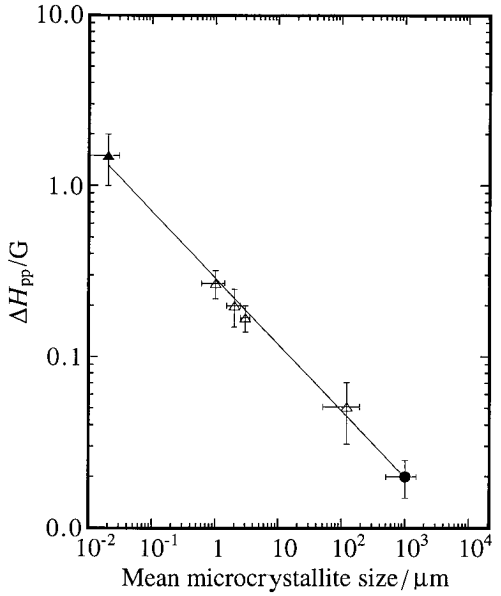

Fig. 3 Correlation between the peak-to-peak EPR signal linewidth ΔH_{pp}, measured under vacuum, and the mean length $\langle l \rangle$ of x-PcLi microcrystallites in various systems: (▲) electrodeposited films obtained for different electrolysis times, (◇) x-PcLi film obtained by vacuum evaporation and (●) x-PcLi single crystal. The continuous line is the result of a power-law fit, $\Delta H_{pp} = K\langle l \rangle^{\alpha}$ with $\alpha \approx 0.36 \pm 0.04$.

EPR signal are strongly dependent on the electrolysis time t_e. As a general tendency, we observed that with increasing mean microcrystallite size $\langle l \rangle$ and increasing unidirectional order in the films, the EPR signal linewidth ΔH_{pp} progressively decreased.

The relation between the EPR signal linewidth under vacuum ΔH_{pp} and the mean size of the microcrystallites forming the films is depicted in Fig. 3, for different systems: (i) electrodeposited x-PcLi thin films grown in acetonitrile for different electrolysis times t_e, (ii) a 50 nm x-PcLi film obtained by vacuum deposition onto a glass substrate[2] and (iii) an x-PcLi single crystal obtained by electrosynthesis.[1] For electrodeposited thin films, the mean size of the microcrystallites was obtained by means of a statistical study of SEM micrographs as reported in ref. 10. For a given film, the resulting EPR signal is the sum of the various contributions arising from the narrow microcrystallite size distribution.

We can clearly see that ΔH_{pp} follows a power law of the mean microcrystallite size $\langle l \rangle$ according to the equation $\Delta H_{pp} \propto \langle l \rangle^{\alpha}$ with $\alpha = 0.36 \pm 0.04$. The effect of the electrolysis time on the EPR signal linewidth is probably related to the efficiency of the EPR signal narrowing, *i.e.* to the delocalization and/or the diffusive motion of the spins along the stacking direction in the microcrystallites. This narrowing mechanism is particularly sensitive to chain interruptions along the stacking axis. These mesoscopic effects may have different origins, such as: (i) the occurrence of a structural transformation with increasing t_e, (ii) the presence of chemical impurities and trapped oxygen in the microcrystallites, (iii) the presence of crystallographic defects and (iv) the effect of the limited microcrystallite size on the narrowing mechanism of the EPR signal.

Firstly, the observed linewidth variation does not correspond to any phase transformation, as observed in the case of vacuum deposited thin films grown at different substrate temperatures, since the x structure of PcLi is always evidenced by X-ray diffraction[10] and the apparent spin $S = 1/2$ concentration remains typical of x-PcLi (0.1–0.05 spins per molecule).[4] However, we cannot exclude the possibility that the observed linewidth variation of the EPR signal is related to a continuous structural transformation consisting of a progressive variation of the unit cell parameters with increasing size of the microcrystallites. Indeed, in our previous study, we demonstrated that the interstack parameter $d_{100}{}^{x}$ increases slightly with increasing t_e, *i.e.* with increasing mean microcrystallite size $\langle l \rangle$, between $d_{100}{}^{x} = 1.376$ nm when $t_e = 1$ min ($\langle l \rangle \approx 2$ μm) and $d_{100}{}^{x} = 1.41$ nm when $t_e = 10$ min ($\langle l \rangle \approx 20$ μm).[10] Moreover, the interstack parameter observed in vacuum deposited x-PcLi thin films is found in the range 1.36–1.38 nm, with the typical size of the domains being in the region of a few tens of nm.[2]

Secondly, if we assume that the amount of oxygen trapped in the microcrystallites is responsible for the observed modification of the EPR signal linewidth, one should observe different magnetic characteristics for the films depending on the preliminary degassing of the $PcLi_2$ solution. However, no obvious differences in the magnetic properties of electrodeposited thin films were evidenced as a function of degassing.

Crystallographic defects have been clearly observed in phthalocyanine thin films by high resolution transmission electron microscopy (HRTEM) and are surely one of the major origins for the spin localisation in x-PcLi, as demonstrated for vacuum deposited thin films.[9,11] The study of morphology in electrodeposited thin films by SEM has clearly demonstrated that the shape of microcrystallites with a size below 1 μm is not well defined, in particular, the edges of the crystallites are not sharp and suggest the presence of a high concentration of crystallographic defects. Murata *et al.* have demonstrated the presence of highly disordered regions surrounding the microcrystallites in various phthalocyanine thin films.[11] The influence on the spin dynamic of these disordered regions may reasonably be assumed to be much more important in the case of small crystallites with a size below 1 μm.

The last possible origin for the mesoscopic effects on the EPR signal linewidth is the dependence of the signal narrowing mechanism on the size of the microcrystallites. It is well known that the narrowing of the EPR signal is related to the delocalization and/or diffusion of spin excitations and also to the dimensionality of the systems, the narrowing being more effective in a 3D system than in a 1D system. However, in the case of x-PcLi, a typical 1D spin diffusion was calculated from the linewidth anisotropy (see section 3.1.3) which therefore suggests that the efficiency of the narrowing mechanism is related to the mean length of the PcLi stacks in the crystallites, *i.e.* to the mean length of the microcrystallites. Accordingly, we expect narrowing of the EPR signal to be most efficient in large crystallites of macroscopic size and much less in microcrystallites with a size below 1 μm. This latter assumption however, requires that the spin excitations are highly mobile and/or delocalized over distances up to several microns. It must be stressed that no such mesoscopic effects on the EPR signal linewidth have so far been observed and that no theoretical framework has been proposed. A tentative analysis of the results in terms of the hyperfine contribution to the EPR line which is related to the spin density distribution would lead to a relation of the type $\Delta H_{1/2} \propto \langle l \rangle^{-1/2}$ which differs significantly from our experimental result.

For most of the electrodeposited thin films, we observed that the EPR signal is asymmetric and that its asymmetry depends on the mean size of the microcrystallites. As shown in Fig. 2, the EPR signal asymmetry is most pronounced for the films obtained when $t_e = 2$ min, which show microcrystallites with mean sizes of *ca.* 2–3 μm, and tends to disappear for films where the microcrystallite size is in the order of several hundreds of microns ($t_e \approx 15$–30 min) and also for the films obtained when $t_e < 10$ s. This variation of the EPR signal asymmetry as a function of the mean microcrystallite size may be interpreted in terms of two different components of the EPR signal which are probably related to two exchange coupled spin species corresponding to localized spins, as observed in vacuum deposited thin films, and delocalized/

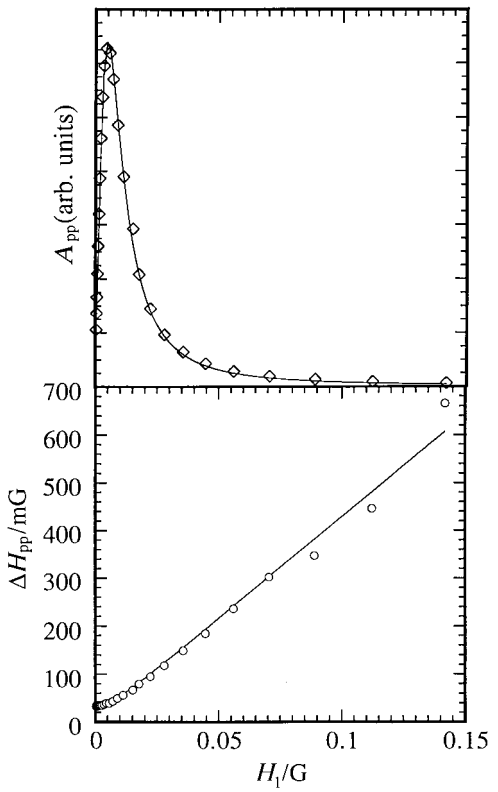

Fig. 4 Peak-to-peak amplitude $[A_{pp}(H_1)]$ and peak-to-peak linewidth $[\Delta H_{pp}(H_1)]$ saturation curves for an x-PcLi thin film of thickness *ca.* 2 μm obtained *via* electrodeposition onto an ITO substrate in acetonitrile ($t_e = 30$ min.). The sample was kept under vacuum and oriented at the magic angle to the Zeeman field. The continuous lines represent fits using the theoretical expressions for $A_{pp}(H_1)$ and $\Delta H_{pp}(H_1)$ in the case of a Lorentzian line shape.

diffusing spins, as observed in x-form single crystals. Further support for the latter assumption is obtained in Section 3.2 from the study of the temperature dependence of the EPR signal.

The electrolysis time or, equivalently, the mean microcrystallite size in the films also affects the saturation characteristics of the corresponding EPR signal. As seen in Fig. 4, thin films obtained when $t_e = 30$ min in acetonitrile exhibit a saturation behaviour of the peak-to-peak amplitude A_{pp} and linewidth ΔH_{pp} (at the magic angle, *i.e.* $\theta = \pm 55°$) which is typical for a pure Lorentzian line. The values derived from the saturation experiments for the relaxation times T_1 and T_2 are *ca.* 27 μs and 2.5 μs, respectively. These values are nearly identical to those derived from saturation experiments in the case of x-PcLi single crystals, where $T_1 = 28$ μs and $T_2 = 2.6$ μs.[4] The product T_1T_2 for films corresponding to different t_e show that both the spin–spin relaxation time T_2 and the spin–lattice relaxation time T_1 tend to decrease with decreasing electrolysis time, *i.e.* decreasing mean size of the microcrystallites (Table 1).

In summary we can state that the magnetic properties of electrodeposited x-PcLi thin films obtained when $t_e < 1$ min are similar to those observed in vacuum evaporated films, *i.e.* they are characteristic of a random distribution of microcrystallites in the substrate plane. Conversely, the well oriented films obtained when $t_e > 10$ min show a high degree of unidirectional ordering and behave like x-PcLi single crystals.

3.1.2 Effect of the solvent. As reported in the case of powders, the solvent used during electrosynthesis is a key factor affecting the magnetic properties of x-PcLi. Films grown in acetone behave quite differently from those grown in acetonitrile (Table 1). Firstly, the EPR signal under ambient atmosphere is quite narrow for the thin films grown in acetone (thickness *ca.* 1–2 μm) with a typical linewidth of about 150 mG ($t_e = 8$ min) *versus* 1.0–1.2 G for films grown in acetonitrile. This observation suggests that the oxygen molecules which are responsible for the signal broadening cannot diffuse easily in the microcrystallites grown in acetone. The same effect of the solvent on the magnetic properties of x-PcLi has already been observed for powders grown in acetone and was interpreted in terms of a distorted x-PcLi structure because of the presence of occluded solvent molecules in the microcrystallites.[2] If the diffusion of molecular oxygen is indeed less efficient in x-PcLi grown in acetone because of structural defects, we would expect the coexistence of two spin populations corresponding to spins located in regions without oxygen (spin A) and spins in contact with oxygen (spin B), *i.e.* a narrow (20–30 mG) and a broad (*ca.* 1 G) contribution to the EPR signal. The absence of such distinct contributions indicates an efficient exchange interaction which can be considered as an argument for the existence of high spin mobility and/or delocalisation. The presence of these two spin populations in the EPR signal is however supported by the saturation behaviour of the EPR signal depicted in Fig. 5. The interesting point is that, regardless of the microcrystallites curving, their mean size seems to have a similar effect on the EPR signal linewidth as mentioned previously for films grown in acetonitrile (Table 1).

3.1.3 Spin dynamics as a function of the electrolysis time. Let us first consider the evolution of the EPR signal anisotropy when the samples are rotated around an axis perpendicular to the preferential growth direction (*c* axis) as depicted in Fig. 6 (films grown in acetonitrile). Whatever the microcrystallite size and the solvent used during the film growth, a clear anisotropy of the linewidth is observed for electrolysis times down to 1 min. In all cases, the maximum linewidth appears when the preferential growth direction of the microcrystallites (*c* axis) is parallel to the Zeeman field B_0.

In order to get some information about the dimensionality of spin diffusion in the thin films, we have applied all the angular dependences of the peak-to-peak EPR linewidth $\Delta H_{pp}(\theta)$ to the expression proposed in the case of x-PcLi single crystals and thin films sublimed onto glass substrates eqn. (1):[9]

$$\Delta H_{1/2}(\theta) = a + bF_0^2(\theta) + c[10F_1^2(\theta) + \frac{1}{\sqrt{2}}F_2^2(\theta)] \qquad (1)$$

with the dipolar contributions $F_0(\theta) = 3\cos^2\theta - 1$, $F_1(\theta) = \cos\theta \sin\theta$ and $F_2(\theta) = \sin^2\theta$.

The low dimensional spin diffusion is derived in this model by assuming a spectral density of $1/\sqrt{\omega}$ which fixes the relative weights of the two non-secular terms $F_1(\theta)$ and $F_2(\theta)$.[12] From a structural standpoint, the existence of low dimensionality in x-PcLi is supported by the columnar arrangement of the molecules which leads to strong molecular orbital overlaps along the stacking direction (intermolecular distance of *ca.* 0.321 nm). Moreover, the validity of this expression has previously been demonstrated for vacuum deposited thin films consisting of needle shaped microcrystallites randomly oriented in the plane of the substrate.[9]

As can be seen from Fig. 6 and Table 2, the contribution of the secular term $F_0(\theta)$, reflecting the low dimensionality of the spin diffusion, is predominant in the films showing the largest microcrystallites and the highest degree of unidirectional ordering. The linewidth anisotropy corresponding to the best oriented thin films is quite similar to that observed for x-form PcLi single crystals.

The low dimensionality of the spin diffusion is also demonstrated by the evolution of the EPR signal lineshape with the orientation of the thin films in the Zeeman field. In Fig. 7 the

Table 1 EPR data at 300 K in ambient atmosphere and primary vacuum for PcLi thin films electrodeposited onto ITO substrates, obtained for various electrolysis times and grown in different solvents

Electrolysis time	Mean size of microcrystallites $\langle l \rangle$/μm	ΔH_{pp}^{vac}/mG	ΔH_{pp}^{air}/mG	$\mu = \Delta H_{pp}^{air}/\Delta H_{pp}^{vac}$	T_1T_2/μs^2
Films grown in CH_3CN					
5 s	1	320	1200	3.8	—
20 s	3	150	1100	7.3	—
1 min	10	90–120	900–1000	10	6.2
2 min	50	45–70	900–1000	13–22	32
16 min	>500	17–30	900–1000	33–60	68±5
Films grown in $(CH_3)_2CO$					
1 min	3	140	330	2.4	—
2 min	5	64	200	3.1	—
8 min	20	36	140	3.9	—
Vacuum deposited film[a]	0.02–0.05	800–1000	1800	2	0.15
Single crystal[6]	1000	22–26	1000	38–45	73

[a]The film was obtained on a glass substrate at a substrate temperature of *ca.* 300 K.[9]

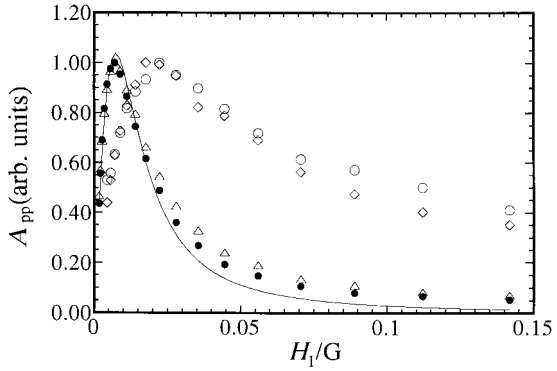

Fig. 5 Peak-to-peak amplitude [$A_{pp}(H_1)$] saturation curves for x-PcLi thin films obtained *via* electrodeposition onto an ITO glass substrate in acetone for increasing electrolysis times: (○) t_e=30 s, (◇) t_e=1 min, (△) t_e=2 min and (●) t_e=8 min. The samples were kept under vacuum and oriented at the magic angle. The continuous line represents the fit using the theoretical expressions for $A_{pp}(H_1)$ and $\Delta H_{pp}(H_1)$ in the case of a Lorentzian line shape.

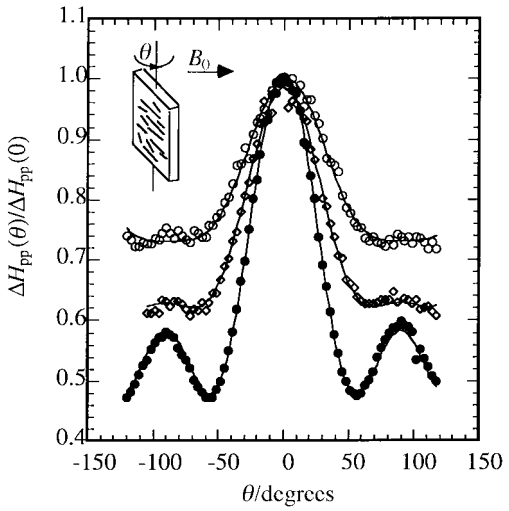

Fig. 6 Angular dependence of the normalized linewidth anisotropy at 300 K for x-PcLi thin films obtained *via* electrodeposition onto ITO glass substrates in acetonitrile for various electrolysis times: (○) t_e=1 min [$\Delta H_{pp}(0) \approx 140$ mG], (◇) t_e=2 min [$\Delta H_{pp}(0) \approx 100$ mG] and (●) t_e=16 min [$\Delta H_{pp}(0) \approx 30$–50 mG]. All the samples were kept under primary vacuum. The data have been fitted using eqn. (1) (see text). The inset shows the orientation of the sample in the Zeeman field. The maximum linewidth was observed when the preferential growth direction (*c* axis) was parallel to the Zeeman field (θ=0°).

Table 2 Parameters obtained after fitting of the EPR linewidth anisotropy according to eqn. (1) for electrodeposited x-PcLi thin films grown in acetonitrile onto ITO substrates over various electrolysis times. In order to increase the signal to noise ratio, the linewidth anisotropy was calculated from the peak-to-peak amplitude (Fig. 6). The EPR linewidth is derived from the peak-to-peak amplitude by using the approximation $\Delta H_{1/2} \approx 1/\sqrt{A_{pp}}$

Sample (electrolysis time/min)	*a*/mG	*b*/mG	*c*/mG	*b*/*a*	*c*/*a*
1	90–120	17–23	12–16	0.19	0.13
2	45–70	15–23	9–13	0.33	0.19
20	17–30	6–11	1–2	0.36	0.06

intensity of the EPR signal corresponding to an x-PcLi thin film obtained when t_e=20 min in acetonitrile is plotted for different orientations in the Zeeman field in the form I_0/I *vs.* $(H-H_0)^2/\Delta H_{1/2}{}^2$. An obvious change of the signal line shape with orientation was observed, the signal being Lorentzian only for $\theta = \pm 55°$. Using the approach proposed by Hennessy *et al.*,[13] the value of the ratio $\alpha = J'/J$ between the interchain exchange interaction J' and the intrachain exchange interaction J can be obtained from the data of Fig. 7. Assuming a purely uniaxial system in agreement with the structural data of x-PcLi,[3] gives $\alpha \leqslant 10^{-3}$. Accordingly, the anisotropy of the spin

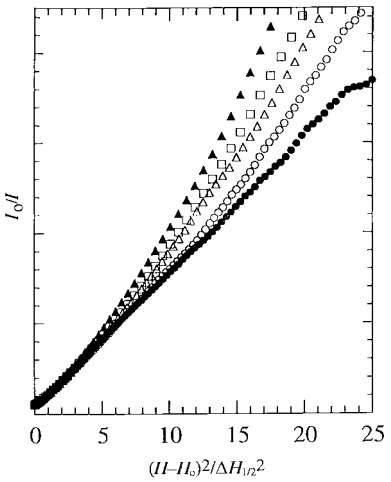

Fig. 7 Angular dependence of the EPR signal line shape for an electrodeposited x-PcLi thin film obtained in acetonitrile when t_e=20 min: (▲) θ=0°, (□) θ=9°, (△) θ=18°, (○) θ=36° and (●) θ=55°. All the spectra were recorded under vacuum using the field frequency lock in order to avoid any distortion of the narrow EPR signal.

diffusion, defined as $\beta=\tau_t/\tau_c$, can be derived with eqn. (2):

$$\tau_t^{-1}=(J'/\hbar)[(J'/\hbar)\tau_c]^{1/3} \quad (2)$$

where τ_t is the characteristic transverse correlation time, and eqn. (3)

$$\tau_c^{-1}=J/\hbar \quad (3)$$

where τ_c is the intra-chain correlation time.

From these an estimated lower value for β of *ca.* 10^4 can be obtained, which clearly illustrates the low dimensional spin diffusion in electrodeposited thin films of x-PcLi.

The anisotropy of the EPR signal has also been checked in the plane perpendicular to the direction of preferential growth, with the films being rotated around the *c* axis as depicted in Fig. 8. In the case of a perfect unidirectional orientation of all the microcrystallites along the *c* axis, we would not expect any EPR signal anisotropy since x-PcLi single crystals show an isotropic magnetic behaviour in the plane perpendicular to the *c* axis. In the present case, we observed such an anisotropy which is, however, much smaller in amplitude (16%) with respect to that observed when the sample is rotated as shown in Fig. 6 (55%). The latter anisotropy indicates the misalignment of some microcrystallites relative to the *c* axis. In fact, we observe that the larger the mean microcrystallite length, the higher their degree of preferential unidirectionnal ordering along the *c* axis and the smaller the EPR signal anisotropy in the plane perpendicular to the *c* axis. For films with thickness of less than 50 nm, *i.e.* films showing no unidirectional ordering of the crystallites, we observed the same linewidth anisotropy regardless of the rotation axis in the plane of the ITO substrate. The latter situation is identical to that observed for vacuum deposited thin films which consist of needle-shaped microcrystallites randomly oriented in the plane of the substrate.

In addition to the linewidth anisotropy, we observe a small but significant *g*-factor anisotropy at 300 K for the best oriented x-form thin films. A relative *g*-factor variation of *ca.* $\Delta g=g_{\parallel}-g_{\perp}=4\times10^{-5}$ corresponding to a resonant field shift of *ca.* 50–80 mG, *i.e.* 2–4 times the linewidth of the EPR signal is observed. The amplitude of this resonant field shift is nevertheless much smaller with respect to the EPR signal linewidth observed for films obtained when $t_e<1$ min. Accordingly, the EPR signal broadening observed with decreasing t_e, *i.e.* decreasing microcrystallite size, is not merely related to the difference in the unidirectional orientation degree of the microcrystallites, but implies some drastic size effects as already discussed in Section 3.1.1.

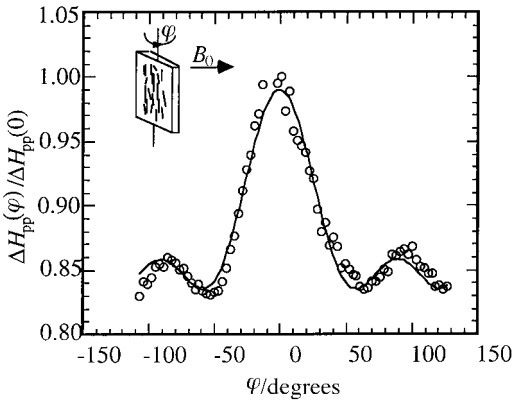

Fig. 8 Angular dependence of the linewidth anisotropy at 300 K for an electrodeposited x-PcLi thin film grown in acetonitrile onto an ITO substrate (thickness 2 μm, $t_e=30$ min). The sample was kept under vacuum and rotated around the *c* axis (preferential growth direction) as shown in the inset. The data have been fitted using eqn. (1) (see text).

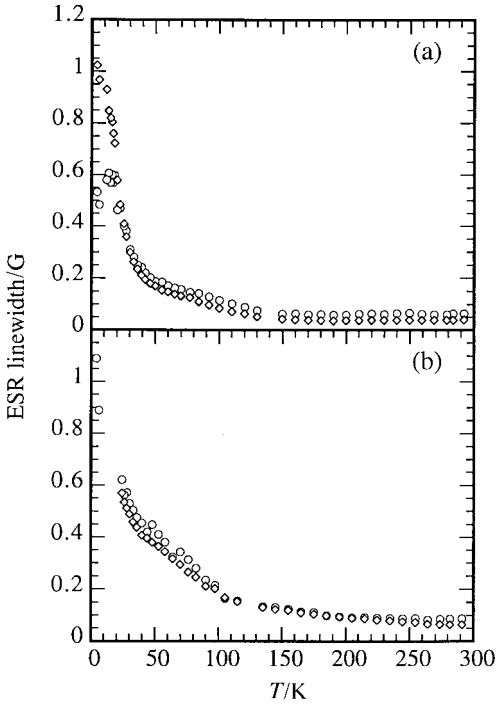

Fig. 9 Temperature dependences of the EPR signal linewidths [$\Delta H_{1/2}$ (◇) and ΔH_{pp} (○)] for an electrodeposited PcLi thin film grown in acetonitrile onto an ITO substrate (thickness *ca.* 2 μm, $t_e=30$ min): (a) sample sealed under vacuum at 10^{-4} mbar and (b) sample kept in a sealed tube under 35 mbar O_2. The sample was oriented such that the *c* axis was parallel to the Zeeman field.

3.2 Temperature dependence of the magnetic properties

3.2.1 EPR signal line shape and linewidth. The line shape of the EPR signal for well oriented x-form thin films obtained in acetonitrile does not show any discontinuous modification with temperature and always remains quite close to a Lorentzian line. As seen in Fig. 9, the EPR signal half-linewidth at half maximum $\Delta H_{1/2}$ initially remains nearly constant with decreasing temperature until 100 K. Below this temperature, $\Delta H_{1/2}$ starts increasing until it reaches a saturation value of about 1.0–1.3 G at 4 K. However, we also observed that the peak-to-peak linewidth ΔH_{pp} clearly behaves differently from $\Delta H_{1/2}$ below *ca.* 20 K. Indeed, while $\Delta H_{1/2}$ continues to increase, ΔH_{pp} starts decreasing slightly with decreasing temperature. This behaviour of ΔH_{pp} and $\Delta H_{1/2}$ indicates the presence of two contributions to the EPR signal, most likely corresponding to diffusing and trapped spin species, as proposed previously to explain the signal anisotropy observed at 300 K. In order to observe one single line in the EPR spectrum, the exchange frequency, $J_{\pi loc}$, between the localized states and the diffusive states has to be larger than $(g_{loc}-g_{\pi})\mu_B B_0$, where g_{loc} and g_{π} are the *g*-factors for the localized and diffusive spins.[14] This relation holds until $T\approx10$ K, when the two components are clearly evidenced.

3.2.2 Magnetic susceptibility. The behaviour of the magnetic susceptibility has been studied for electrodeposited PcLi thin films grown in acetonitrile with thicknesses of *ca.* 2 μm (Fig. 10). In particular, we have studied the effect of molecular oxygen on the magnetic susceptibility.

In the same way as for PcLi x-form powders, the susceptibility can be fitted by means of two components consisting of an activated contribution and a simple Curie–Weiss contribution. These two contributions to the magnetic susceptibility have previously been attributed to two independent spin populations, namely diffusive spins giving rise to the activated contribution to the total susceptibility $\chi(T)$ and localized spins characterized by a Curie–Weiss contribution.[4] The spin popu-

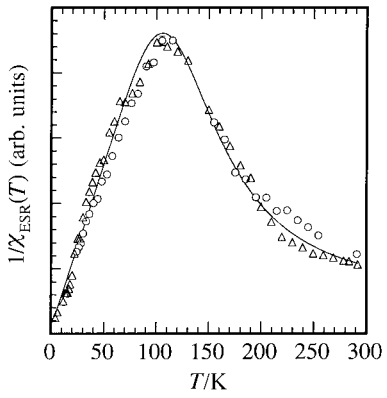

Fig. 10 Temperature dependence of the reciprocal EPR susceptibility of an electrodeposited x-PcLi thin film grown in acetonitrile (thickness *ca.* 2 μm, $t_e = 30$ min): (△) sample sealed in a quartz tube under vacuum (10^{-4} mbar) and (○) in the presence of 35 mbar pure oxygen. The magnetic susceptibility has been fitted using the expression proposed in ref. 4(*a*) for x-PcLi powders. The reciprocal susceptibility curves are normalized to the maximum value observed which occurs at *ca.* 100 K.

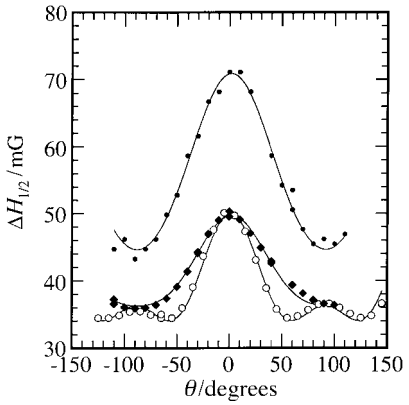

Fig. 11 Angular dependence of the linewidth anisotropy for an x-form PcLi thin film of thickness 2 μm ($t_e = 30$ min) obtained *via* electrodeposition onto an ITO substrate in acetonitrile obtained at various temperatures: (○) 300 K, (◆) 200 K and (●) 140 K. The sample was kept under secondary vacuum in a sealed quartz tube.

lation responsible for the activated component has previously been attributed to the conduction electrons, despite the clear disagreement between the activation energy of the susceptibility and the dc conductivity.[4,15] The Curie–Weiss contribution was assigned to the localised spin states associated with intrinsic structural defects rather than to the presence of residual oxygen trapped in the microcrystallites.

As for powders and single crystals, the contribution of the activated component is dominant when $T > 100$ K. The activation energy of *ca.* 0.059 eV (705 ± 25 K) is slightly larger than that observed in powders [$E_A(\chi) \approx 0.042$ eV]. In all cases, this activation energy is quite different from that observed for the dark conductivity, $E_A(\sigma)$, in compacted powders and single crystals, where $E_A(\sigma) \approx 0.14$ eV and $E_A(\sigma) \approx 0.10$–0.20 eV, respectively, indicating a clear separation between spin and charge excitations.[4,15]

When $T < 100$ K, the Curie–Weiss component of the susceptiblity becomes dominant, the corresponding coupling constant T_{CW} hints at small antiferromagnetic couplings, with T_{CW} being *ca.* -1.6 ± 1 K ($t_e = 30$ min) *versus* -3 ± 1 K in x-PcLi powders. From the fitting of the susceptibility it is seen that the ratio between the Curie constants of the localized and activated contributions is of the order of 0.8%. Therefore, we consider that the activated spin population characterizes the intrinsic magnetic properties of x-PcLi. As reported previously, the Curie–Weiss contribution to the total susceptibility is probably associated to the trapped/localized spin states, also evidenced by the linewidth behaviour below 100 K.

In order to highlight the role of oxygen on the temperature dependence of the susceptibility, we have recorded the EPR susceptibility of a thin film in the presence of 35 mbar pure O_2 (Fig. 10). Our results indicate that the magnetic susceptibility is not altered by the presence of oxygen in the temperature range 20–300 K, even if the linewidth shows some differences in the range 20–100 K. The relative consentration of the Curie–Weiss and activated spin populations is unaffected by the introduction of oxygen in the samples. This observation demonstrates the 'intrinsic' nature of the Curie–Weiss spin population which is most likely due to spins trapped by structural defects.

3.2.3 Evolution of the spin dynamic with temperature. The temperature dependence of the linewidth anisotropy for a film of thickness 2 μm is shown in Fig. 11, the corresponding fitting parameters are collected in Table 3.

In the temperature range 140–300 K, a low dimensional spin diffusion is still observed since the contribution of the secular term $F_0(\theta)$ remains dominant even though it clearly decreases with temperature (Table 3). Consequently, the linewidth minima corresponding to the magic angles $\theta = \pm 55°$ are progressively shifting towards $\theta = \pm 90°$. Also interesting is the fact that the hyperfine contribution to the EPR signal in eqn. (1) remains constant ($a \approx 30$ mG) down to 140 K, supporting the validity of the model proposed for the 1D spin diffusion in this system. Below 140 K, no further important variations in the overall linewidth anisotropy are observed: it is dominated by the trapped nature of the spin excitations, as deduced from the linewidth temperature modelling. Accordingly, below 140 K, the 1D diffusive character of the spin excitations disappears progressively at the expense of the 3D behaviour, which is characteristic of trapped spin states.

Table 3 Parameters obtained after fitting of the EPR linewidth anisotropy in the temperature range 140–300 K using eqn. (1) for an electrodeposited film of x-PcLi (film thickness *ca.* 2 μm, $t_e = 30$ min, solvent: acetonitrile). The film was maintained under vacuum (10^{-4} mbar) in a sealed quartz tube

T/K	a/mG	b/mG	c/mG	b/a	c/a
300	30	4.9	1.5	0.16	0.05
200	28	5.5	4.4	0.20	0.16
140	27	11	10	0.41	0.37

3.3 Effect of oxygen

3.3.1 Effect of oxygen at 300 K. The effect of oxygen on the magnetic properties of x-form PcLi has been extensively studied in the case of several x-PcLi systems, such as single crystals, powders and thin films obtained by vacuum deposition.[2,9] In these systems, the oxygen sensitivity of the films was found to be very small ($\Delta H_{pp}^{air}/\Delta H_{pp}^{vac} \approx 2$ and $\Delta H_{pp}^{vac} \approx 0.8$–$1.0$ G for x-PcLi thin films deposited onto glass substrates at 300 K) owing to a pronounced localization of the spins due to the disorder and the reduced size of the microcrystalline domains (of the order of a few tens of nm for PcLi thin films deposited at 300 K onto glass substrates).[2,9]

The EPR signal of an electrodeposited x-PcLi thin film (thickness *ca.* 2 μm) exhibits a linear dependence of the EPR signal linewidth on oxygen pressure between $\Delta H_{pp} =$ 20–30 mG, when under vacuum, and 1.1 G under ambient oxygen pressure ($P_{O_2} \approx 200$ mbar, Fig. 12). The corresponding sensitivity factor of the films, defined as $d(\Delta H_{pp})/d(\Delta P_{O_2})$, is almost identical to that reported for powders and single crystals.[5] Nevertheless, contrary to the case of *trans*-polyacetylene, the linewidth broadening with oxygen is not accompanied by a corresponding change in the dc conductivity,

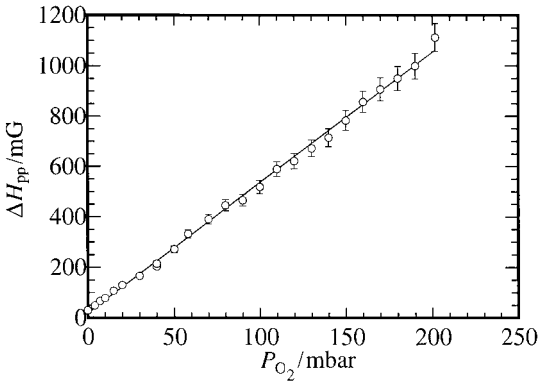

Fig. 12 Dependence of the EPR signal linewidth on the partial pressure of O_2 for an electrodeposited x-PcLi thin film grown in acetonitrile (thickness *ca.* 2 μm, $t_e = 30$ min). The continuous line is the result of a linear fit of the experimental data.

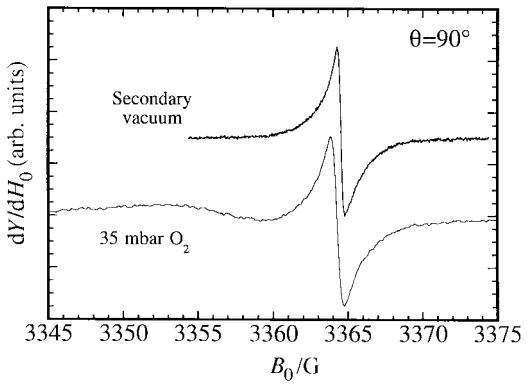

Fig. 13 EPR signal at 4 K for an electrodeposited x-PcLi thin film grown in acetonitrile (thickness 2 μm, $t_e = 30$ min): (a) sample in a sealed quartz tube (10^{-4} mbar) and (b) under 35 mbar oxygen. The sample was oriented with the preferential growth direction of the crystallites (*c* axis), perpendicular to the Zeeman field.

indicating that the interaction between molecular oxygen and PcLi is purely magnetic and does not involve any charge transfer mechanism.[13] The kinetics of the oxygen effect are identical to those observed in powders and single crystals[2] with characteristic time constants of a few seconds. No significant difference between the sorption and desorption kinetics is evidenced. The oxygen sensitivity of the films depends on the electrolysis time, *i.e.* on the mean size of the microcrystalline domains: the smaller the microcrystallites, the smaller the sensitivity factor μ (Table 1). However, since the linewidth measured under 200 mbar O_2 does not depend on the sample ($\Delta H_{pp}^{air} \approx 0.9$–$1.2$ G), the reduced oxygen sensitivity observed in the films obtained when $t_e < 1$ min is merely a consequence of the larger EPR linewidth observed under vacuum. It also appears that the kinetics of the oxygen effect do not change drastically with the mean microcrystallite size. The oxygen sensitivity of PcLi thin films grown in acetone is much smaller compared to that observed for films grown in acetonitrile, since the EPR signal of the former is also narrow under an ambient oxygen atmosphere (Table 1).

3.3.2 Oxygen effect at low temperature. In a previous study, we reported the important effect of oxygen on the magnetic properties of β-form PcLi needles at low temperature, showing that the EPR signal is strongly altered below 55 K with one or more additional contributions clearly seen at 4 K.[4]

In order to check the oxygen effect on the magnetic properties, we prepared two samples: (i) a film kept under an atmosphere of 35 mbar pure oxygen and (ii) a film kept in a secondary vacuum. Besides the signal seen in the absence of O_2, a second broad signal ($\Delta H_{pp} \approx 10$ G) located at $g \approx 2.0053$ is observed (Fig. 13). The study of the signal anisotropy indicates that the broad signal behaves isotropically. Accordingly, this signal is believed to arise from randomly distributed and localised spins $S = 1/2$ interacting with the oxygen molecules trapped in the microcrystallites.

The presence of oxygen in the sample also affects the properties of the intrinsic spin species observed in the absence of O_2. Indeed, as seen in Fig. 9, the temperature dependence of the EPR linewidth is altered by the presence of oxygen in the sample. Additionally, we have also observed that the presence of molecular oxygen modifies the *g*-factor of the diffusing spin species at low temperature. Indeed, the amplitude of the *g*-factor anisotropy at 4 K is much larger in the presence of oxygen ($g_{\parallel} - g_{\perp} = 3.5 \times 10^{-4}$ *vs.* $g_{\parallel} - g_{\perp} = 9 \times 10^{-5}$) compared to the case when the sample is conditioned under vacuum. The same kind of behaviour already mentioned in the case of beta-PcLi hints at the presence of magnetic couplings existing between the spins that are trapped by oxygen and the delocalized diffusing spins.

4 Discussion

In this section, we propose to analyze the experimental results obtained for the x-structure of PcLi (temperature dependence of the magnetic susceptibility as well as the EPR signal linewidth) in the frame of a soliton approach as proposed in the cases of galvinoxyl,[16] tetrathiafulvalene–*p*-chloranil[17] and KCP [$K_2Pt(CN)_4Br_{0.3} \cdot 3.2H_2O$].[18]

The theoretical study of $S = 1/2$ spin solitons in one-dimensional (1D) systems, including spin-Peierls systems, has received much interest in the last twenty years,[19] but only a few experimental studies have evidenced spin solitons in molecular organic systems.[16–18] Suzuki, for example, analysed the magnetic properties of charge transfer salts, observed *via* EPR, in terms of spin solitons.[19] To explain the generation of these spin solitons, the author introduces a similar Hamiltonian to that given by Su *et al.*[20] for *trans*-$(CH)_x$, namely a Hamiltonian taking into account the electron-phonon coupling *via* a linear dependence between the magnetic coupling constant *J* and the local deformation of the crystal lattice. This magneto–elastic coupling leads to a dimerization of the chains with the opening of a magnetic band gap Δ separating the antiferromagnetic ground state band from the excited triplet state band. The $S = 1/2$ spin solitons are accordingly described as phase mismatch defects in the antiferromagnetic chains which correspond to states located in the band gap of the system at *ca.* Δ/π above the ground state band. As proposed by Suzuki, these spin solitons are mainly characterized by: (i) a thermally activated susceptibility of activation energy $E_A(\chi) = \Delta/\pi$ and (ii) a temperature dependent motional-narrowing of the EPR linewidth.

Several results obtained from our EPR study are in accord with the main characteristics of spin solitons as proposed by Suzuki in the case of charge transfer salts. Firstly, we have observed that the dominant contribution to the spin susceptibility shows a typical activated behaviour, with an activation energy $E_A(\chi)$ clearly different from that observed for the dc conductivity $E_A(\sigma)$. Acccordingly, in the frame of Suzuki's soliton model, the $S = 1/2$ EPR signal may be interpreted in terms of thermally generated solitons corresponding to states located in the band gap of the semiconductor at *ca.* $2E_a(\chi) = 0.08$–0.12 eV above the fully occupied ground state band (Fig. 14). This interpretation accounts for the difference existing between the activation energy of the dc conductivity $E_A(\sigma)$, corresponding to charge carrier generation, *i.e.* to excitations from the valence to the conduction band, and the activation energy $E_A(\chi)$ of the magnetic susceptibility, related to the soliton generation. Moreover, the ratio between $E_A(\chi)$ and $E_A(\sigma)$ is in the range 2–3.5, *i.e.* close to the theoretical value of π calculated for spin-Peierls systems. The activation energy

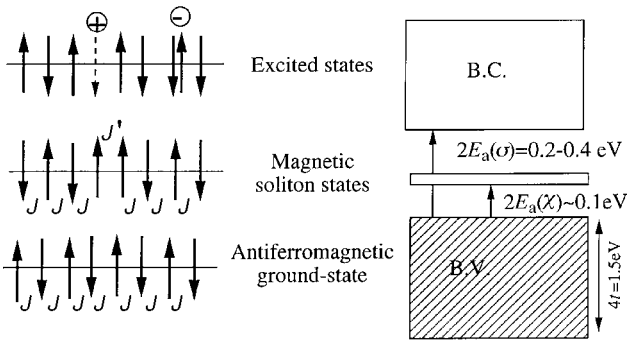

Fig. 14 Schematic drawing of the electronic states involved in the x structure of PcLi assuming a band structure as proposed by Yakushi *et al.*[21] The magnetic soliton is represented as a phase mismatch or a domain wall dividing the antiferromagnetic chain into two segments, each showing different spin alternations.

of the magnetic susceptibility $E_A(\chi)$, *ca.* 0.05–0.06 eV, is also quite similar to that reported for many simple alkali metal-TCNQ salts, such as Rb-TCNQ or K-TCNQ, where $E_A(\chi)$ is typically in the range 0.05–0.08 eV.

The soliton nature of the $S=1/2$ spin excitations in the PcLi x structure is further supported by the fact that the apparent spin concentration is very small (1 spin per 10 to 20 molecules), which is in agreement with the fact that the ground state of the system should be antiferromagnetic, and also with the high value found for the on-site Coulomb repulsion energy U_{eff}, which is *ca.* 1.5 eV.[21] The antiferromagnetic nature of the magnetic couplings in the x structure of PcLi has been clearly ascertained in a previous study,[4] within the framework of Mc Connell's mechanism for the magnetism in solid free π-radicals[22] and on the basis of experimental and theoretical results for the atomic spin density distribution in the PcLi molecule.[23]

As a matter of fact, we also observed that the value of the apparent spin $S=1/2$ concentration at 300 K matches with the corresponding exponential factor in the magnetic susceptibility $\chi(T)=(C/T)\exp(-E_a(\chi)/k_BT)$ with $E_a(\chi)/k_B\approx 714$ K. This implies that the 'Curie constant' C is proportional to the total number of molecules in the sample which in turn implies that the spin observed by EPR can be associated to spin solitons generated in the entire bulk of the crystal. Compared to *trans*-polyacetylene[13,20] and galvinoxyl,[16] where the spin soliton concentrations at 300 K are *ca.* $0.3–1\times10^{-3}$ and 0.3×10^{-3} respectively, we have observed that the spin concentration is much larger in PcLi, which may imply the existence of strong correlations between the soliton-like excitations, especially in the case of a significant extension of the individual solitons of several molecular sites.

It must be stressed that the soliton approach of Suzuki is proposed in the case of a spin-Peierls system characterized by dimerization along the stacking axis. x-PcLi differs from a true spin-Peierls system in the sense that no dimerization of the stacks has been evidenced (all the intermolecular distances in a stack are identical[21]) and no triplet state is observed *via* EPR. However, the x structure of PcLi is such that the unit cell contains two non equivalent molecules along the stacking axis[3] resulting in a doubling of the periodicity along that axis in a similar manner as for a true spin-Peierls system after dimerization. We therefore believe that the soliton approach to the analysis of the magnetic properties of charge transfer salts can reasonably be applied to the case of PcLi.

5 Conclusion

The magnetic properties of x-PcLi thin films grown *via* electrodeposition onto ITO glass substrates in acetone and acetonitrile have been studied *via* EPR. Our investigations demonstrate the presence of some drastic mesoscopic effects affecting the magnetic properties of the x structure of PcLi. By tuning the electrolysis time, it is possible to control the mean size of the microcrystallites as well as their preferential unidirectional ordering in the plane of the substrate. We have demonstrated that the magnetic characteristics of well oriented x-form PcLi thin films with thicknesses of *ca.* 2 μm, obtained by electrodeposition onto ITO glass substrates, are quite similar to those observed for single crystals: a narrow EPR signal, with a linewidth down to 17 mG, which broadens linearly with the oxygen pressure is observed in the best oriented films.

A qualitative analysis of the magnetic properties of x-PcLi in terms of magnetic solitons is proposed. The temperature dependence of the susceptibility and the EPR linewidth as well as the activated nature of the dc conductivity are modelled in the frame of a solution model. The solitons consist of phase-mismatch defects in the spin alternation of the antiferromagnetic chains of PcLi molecules and are generated thermally with a typical activation energy of *ca.* 40–60 meV. The existence of drastic size effects on the EPR signal linewidth, associated to the characteristic 1D behaviour of the EPR linewidth anisotropy, supports the viewpoint of highly delocalized and/or diffusive spin excitations.

Acknowledgments

Support by EEC contract (CHRX-CT94–0558) and CNRS (MRES grant) for one of us (M. B.) is gratefully acknowledged. We thank Dr P. Turek for stimulating discussions and M. Bernard for technical support.

References

1 (*a*) P. Turek, J.-J. André, A. Giraudeau and J. Simon, *Chem. Phys. Lett.*, 1987, **134**, 471; (*b*) P. Turek, P. Petit, J.-J. André, J. Simon, R. Even, B. Boudjema, G. Guillaud and M. Maitrot, *J. Am. Chem. Soc.*, 1987, **109**, 5119.
2 M. Brinkmann, C. Chaumont, H. Wachtel and J.-J. André, *Thin Solid Films*, 1996, **283**, 97.
3 (*a*) H. Sugimoto, M. Mori, H. Masuda and T. Taga, *J. Chem. Soc., Chem. Commun.*, 1986, 962; (*b*) M. A. Petit, T. Thami and R. Even, *J. Chem. Soc., Chem. Commun.*, 1989, 15; (*c*) H. Homborg and Chr. L. Teske, *Z. Anorg. Allg. Chem.*, 1985, **527**, 45.
4 (*a*) M. Brinkmann, P. Turek and J.-J. André, *J. Mater. Chem.*, 1998, **8**, 675; (*b*) P. Turek, J.-J. André, M. Moussavi and G. Fillion, *Mol. Cryst. Liq. Cryst.*, 1989, **176**, 535.
5 (*a*) P. Turek, J.-J. André and J. Simon, *Solid State Commun.*, 1987, **63**, 741; (*b*) F. Bensebaa and J.-J. André, *J. Phys. Chem.*, 1992, **96**, 5739; (*c*) D. Duret, M. Moussavi, C. Jeandey and M. Beranger, *Sens. Actuators, B*, 1992, **6**, 266; (*d*) X. S. Tang, M. Moussavi and G. C. Dismukes, *J. Am. Chem. Soc.*, 1991, **113**, 5914.
6 J.-J. André and M. Brinkmann, *Synth. Met.*, 1997, **90**, 211.
7 H. Hoshi, Y. Maruyama, H. Masuda and T. Inabe, *J. Appl. Phys.*, 1990, **68**, 1396.
8 (*a*) H. Wachtel, J.-C. Wittmann, B. Lotz, M. A. Petit and J.-J. André, *Thin Solid Films*, 1994, **250**, 219; (*b*) M. Brinkmann, J.-C. Wittmann, C. Chaumont and J.-J. André, *Thin Solid Films*, 1997, **292**, 192.
9 (*a*) M. Brinkmann, P. Turek and J.-J. André, *Thin Solid Films*, 1997, **303**, 107; (*b*) H. Wachtel, J.-J. André, W. Bietsch and J. U. von Schütz, *J. Chem. Phys.*, 1995, **102**, 5088.
10 M. Brinkmann, S. Graff, C. Chaumont and J.-J. André, *J. Mater. Res.*, 1999, **14**(5), in press.
11 (*a*) Y. Murata, T. Baird and J. R. Fryer, *Nature*, 1976, **262**, 722; (*b*) H. Klapper, M. Kobayashi, T. Kobayashi and K. Sato, in *Organic crystals I*, ed. H. C. Freyhardt and G. Müller, Springer Verlag, Berlin, p. 37.
12 H. Brenner and J.-P. Boucher, in *Physics and Chemistry of Materials and Low Dimensional Structure: Magnetic Properties of Layered Transition Metal Compounds*, ed. L. J. de Jongh, Kluwer, Dordrecht, 1990, vol. 9, p. 323.

13 (*a*) B. R. Weinberger, E. Ehrenfreund, A. Pron, A. J. Heeger and A. G. McDiarmid, *J. Chem. Phys.*, 1980, **72**, 4749; (*b*) M. J. Hennessy, C. D. McElwee and P. M. Richards, *Phys. Rev. B*, 1973, **7**, 930.
14 M. Y. Ogawa, J. Martisen, S. M. Palmer, J. L. Stanton, J. Tanaka, R. L. Greene, B. M. Hoffman and J. A. Ibers, *J. Am. Chem. Soc.*, 1987, **109**, 1115.
15 M. Brinkmann, C. Chaumont and J.-J. André, *Thin Solid Films*, 1998, **324,** 68.
16 K. Awaga, H. Okamoto, T. Mitani, Y. Maruyama, T. Sugano and M. Kinoshita, *Solid State Commun.*, 1989, **71**, 1173.
17 T. Mitani, G. Saito, Y. Tokura and T. Koda, *Phys. Rev. Lett.*, 1984, **53**, 842.
18 (*a*) M. Mehring, O. Kanert, M. Mali and D. Brinkmann, *Solid State Commun.*, 1980, **33**, 225; (*b*) O. Panâ, C. Kessler, C. Filip, L. V. Giurgiu, I. Ursu and M. Mehring, *Appl. Magn. Reson.*, 1997, **12**, 247.
19 N. Suzuki, *Phys. Lett.*, 1982, **89**, 208.
20 (*a*) A. J. Heeger, S. Kivelson, J. R. Schrieffer and W.-P. Su, *Rev. Mod. Phys.*, 1988, **60**, 781 and references therein; (*b*) B. Horovitz, *Phys. Rev. Lett.*, 1981, **46**, 742; (*c*) T. Nakano and H. Fukuyama, *J. Phys. Soc. Jpn.*, 1980, **49**, 1679; (*d*) M. Grabowski, K. R. Subbaswamy and B. Horovitz, *Solid State Commun.*, 1980, **34**, 911.
21 K. Yakushi, T. Ida, A. Ugawa, H. Yamakado, H. Ishii and H. Kuroda, *J. Phys. Chem.*, 1991, **95**, 7636.
22 H. M. Mc Connell, *J. Chem. Phys.*, 1910, **39**, 196.
23 B. Gotschy and G. Denninger, *Mol. Phys.*, 1990, **71**, 169.

Paper 8/09778J